NASA TECHNICAL MEMORANDUM

NASA TM X-52175

NASA TM X-52175

INVESTIGATION OF THE DISCHARGE AND EXHAUST BEAM OF A SMALL ARC PLASMA THRUSTOR

by David N. Bowditch
Lewis Research Center
Cleveland, Ohio

TECHNICAL PAPER proposed for presentation at
Plasmadynamics Conference sponsored by the
American Institute of Aeronautics and Astronautics
Monterey, California, March 2-4, 1966

NATIONAL AERONAUTICS AND SPACE ADMINISTRATION · WASHINGTON, D.C. · 1966

INVESTIGATION OF THE DISCHARGE AND EXHAUST BEAM OF A SMALL ARC PLASMA THRUSTOR

by David N. Bowditch

Lewis Research Center
Cleveland, Ohio

TECHNICAL PAPER proposed for presentation at

Plasmadynamics Conference
sponsored by the American Institute of Aeronautics and Astronautics
Monterey, California, March 2-4, 1966

NATIONAL AERONAUTICS AND SPACE ADMINISTRATION

INVESTIGATION OF THE DISCHARGE AND EXHAUST BEAM OF A SMALL ARC PLASMA THRUSTOR

by David N. Bowditch

Lewis Research Center
National Aeronautics and Space Administration
Cleveland, Ohio

ABSTRACT

A simple, low-power dc magnetic expansion thrustor has been under investigation at NASA Lewis Research Center. An electrical discharge is supported in a axial magnetic field between an annular anode and a centered hollow cathode. The thrustor is typically operated at a magnetic field of 250 G, 0.3 mg/sec mass flow, 2.5 A, and 120 V. Its operation is postulated to be dependent on an essentially quiescent electron gas, which accelerates the ions in a charge-free electric field supported by the electron gas pressure gradient. The electron gas pressure also transmits the thrust from the plasma to the containing thrustor anode, backplate, and magnetic field. The thrustor is very similar to the oscillating electron engine and shares the same method of thrust production as the microwave electron cyclotron resonance devices. It is also believed that the thrust mechanism of this dc magnetic expansion thrustor may be responsible for a significant portion of the thrust of the geometrically similar higher-power MPD arc. The object of the experiments to be discussed in this paper is the investigation of this mechanism of thrust production, by mapping local ion energy and momentum using a new Langmuir calorimetric probe, by determining the plasma potential profiles with an emitting probe, and by measuring electron pressure by means of a Langmuir probe. Good agreement is obtained between gross thrust measured by pendulum thrust stand and integrated ion momentum measurements

E-3345

made in the thrustor exhaust. Emitting probe surveys also showed that the equipotential lines in the plasma are predominantly perpendicular to the magnetic field, indicating that an ambipolar electric field is the main ion accelerating mechanism. Also, the electron force on the B field is calculated from the magnetic field shape and electron pressure measurements, and indicates that about half the thrust is applied to the magnetic field. These results agree with the postulated operation.

INTRODUCTION

A simple low-power dc magnetic expansion thrustor has been under investigation at Lewis Research Center (ref. 1). An electrical discharge is supported in a diverging, axial magnetic field between an annular anode and a centered hollow cathode. The proposed principle of thrustor operation is that the discharge supports a hot, nearly quiescent electron gas, which ionizes and accelerates the propellent in a magnetic nozzle. The collisionless ion acceleration results from a space-charge-free electric field that the plasma itself builds. In the accelerating region, the equal ion and electron charge densities make this electrostatic force on the oppositely charged particles equal and opposite. Thus, through this field, the hot electrons transfer their pressure force to the ions, which comprise essentially all the inertia of the plasma and the momentum of the exhaust. The thrust appears as forces on the thrustor structure and magnetic field, which provide the upstream containment of the electron gas. This operation is very similar to the proposed operation of the oscillating electron engine (ref. 2) and shares the same method of ion acceleration with the microwave electron cyclotron resonance devices (refs. 3 and 4). Also, the thrust mechanism

of this thrustor may be responsible for a significant portion of the thrust of the geometrically similar, higher-power MPD arc (refs. 5 to 10).

There has always been a great deal of difficulty in interpreting the measurements required to determine the performance of plasma engines. Even the thrust stand, which was the one measurement considered beyond question, now measures higher thrust than would be compatible with measured input power and thermal losses (ref. 10). The thrust measurement is probably correct, but the testing environment, tank size, and background density are now suspected of causing distortion of the thrust-producing mechanism. Therefore, to corroborate the measured performance and to verify the proposed method of thrust production, the plasma beam of the magnetic expansion engine was investigated. This engine was desirable for this purpose, because its performance is known to be environment sensitive and its power is low, about 300 watts. This allowed investigation of the beam and the discharge inside the anode without destroying uncooled probes.

APPARATUS

Thrustor

The magnetic expansion thrustor was operated at an easily repeated condition of 260 gauss magnetic field, discharge current of 2.5 amperes at 120 volts, and argon propellant flow of 0.35 milligram per second. This produced a specific impulse of 1100 seconds at a thrust efficiency of 7 percent. Performance of twice this impulse and efficiency has been obtained, but it was not considered sufficiently reproducible for the long periods of time required for the probe surveys. A schematic of the engine is shown in figure 1 along with the probe actuation system. The smallest anode diameter

is 0.0415 meter, and it is flaired to an exit diameter of 0.095 meter. The hollow cathode is a tantalum tube with a 1.9×10^{-4}-meter wall and is coated on its 1.09×10^{-3}-meter inner diameter with a mixture of 53-percent barium oxide, 46-percent strontium oxide, and 1-percent calcium oxide. Part of the argon propellent was introduced through the cathode and the rest through oppositely positioned propellent ports in the anode. The discharge current was controlled be varying the flow through the cathode, which was heated by the discharge. The engine is mounted in a 0.56-meter cubical aluminum box, attached to a large vacuum facility by a 12-inch-diameter valve. At the above operating conditions, the background pressure in the box was 4×10^{-5} torr. The discharge power supply was floating so that the engine discharge sought its own potential, which placed the cathode a few volts above ground. The thrustor is mounted on a pendulum so that its thrust could be determined at anytime by terminating the discharge.

Probes

Two probes were mounted on the actuating system shown in figure 1, which allowed about 0.1-meter axial travel and 90° angular movement. This permitted either detailed surveys inside the thrustor anode with a long probe or measurements up to 0.1 meter in front of the anode with shorter probes. The angular movement of the actuator permitted sampling the exhaust beam only along an arc intersecting the thrustor axis. It was therefore necessary to assume that this traverse was typical of the entire beam.

The discharge was investigated with the three types of probes shown in figure 2, emissive, Langmuir, and Langmuir calorimetric. The emissive probe was used to measure plasma potential. Its voltage was measured by

a 1.5×10^6-ohm voltmeter, and its 5-mil sensing wire was heated by ac current. The wire was heated until further heating produced no change in floating voltage. Domitz (ref. 11) shows this floating voltage to be within a few volts of plasma potential. The Langmuir probe was used in the transition and electron saturation regions to determine electron temperature and number density, which were combined to obtain pressure. The normal reduction assuming quiescent electron gas was used and appeared to work well.

The Langmuir calorimetric probe was made so that the plane Langmuir-probe face could be biased to measure current and thermal power characteristics versus voltage. This was done by gluing a teflon thermal resistance, chosen for its low density, very low heat transfer coefficient, and electrical insulation properties, between a plane Langmuir probe and a water-cooled body. Individual plane probe and guard ring electrical leads allowed separate probe current measurement, and thermal power was measured by determining the temperature drop across the teflon insulator.

The heat capacity of the copper face is easy to determine accurately. The probe time constant is equal to the ratio of the probe face heat capacity and the product of the teflon thermal conductivity and area divided by the teflon thickness. Therefore, the thermal conductivity is calibrated by determining the probe time constant from its measured dynamic response to step changes in heat input. This avoids the problem of accurately determining how much heat enters the probe face during calibration.

REDUCTION OF LANGMUIR CALORIMETRIC PROBE DATA

To interpret the characteristic of thermal power to the probe versus bias voltage, it is necessary to make a heat balance similar to that made

by Compton (ref. 12) when analyzing the cathode of an arc. If the probe is assumed to be in a beam with average directed energy per ion of U_o (eV) and average axial ion velocity of v_o, the ion power density contribution to the surface, after traversing the probe sheath, is

$$P_{ion} = j_i U_o + j_i(\varphi_i - \varphi_\omega) - j_s\varphi_\omega + j_i(V - V_p) \qquad (1)$$

where the beam ion current density $j_i = n_o v_o e$, and n_o is beam number density, φ_i is the ionization potential, φ_ω is the surface work function, j_s is the secondary emission current density, and V and V_p are the probe potential and the plasma potential, respectively. Equation (1) also requires that no collisions occur in the probe sheath and that v_o is larger than the minimum velocity needed for a stable sheath $v_o > \sqrt{\frac{kT_e}{m_{ion}}}$, where T_e is electron temperature in volts, k is the Boltzman constant ($1.602.10^{-19}$ Joules/eV), and m_{ion} is the ion mass. Assuming that the beam is neutral, the beam-directed velocity is small compared with the electron thermal velocity, and the electrons have a Maxwellian distribution, the electron power density to the surface is

$$P_e = j_e(2T_e + \varphi_w) \qquad (2)$$

where the electron current density j_e is

$$j_e = \frac{n_o e}{4}\frac{8kT_e}{\pi m_e}\exp\left[\frac{-e(V - V_p)}{kT_e}\right]$$

and where m_e is the electron mass. The total plasma power density to the probe is, of course, the sum of equations (1) and (2).

To understand the calorimetric data more fully, it is necessary to look at the thermal power variation with probe voltage. The probe power

and current variations with voltage determined in the exhaust of a magnetic expansion plasma thrustor (ref. 1) using argon propellent are presented in figure 3. Since the measured current is constant in the ion saturation region [$-(V - V_p) < 130V$], it can be assumed that the secondary emission is independent of probe potential. Also in this ion saturation region, the electron contribution $P_e A_p$ to the measured power is negligible (where A_p is the probe area). Therefore, it can be seen from equation (1) that the slope of the thermal power curve is equal to the ion current $j_i A_p$ and is 5.5 milliamperes in this case. Comparing this with the measured saturation current of 5.8 milliamperes, which is the sum of the ion and secondary emission currents, determines that the secondary emission current $j_s A_p$ is 0.3 milliampere. The plasma potential V_p was independently determined by the previously discussed emissive probe technique. The product of the ion current with the difference between plasma potential and probe potential determines the ion power gained in the sheath $-j_i A_p(V - V_p)$. The ionization power can be evaluated from the ion current. The power lost to secondary emission for the data of figure 3 is 0.013 watt, which is negligible. Substitution of these powers and the measured power into equation (1) determines that the directed kinetic power $j_i A_p$ is 0.25 watt. Dividing this power by the ion current of 5.5 milliamperes gives a directed kinetic energy per ion of 45.5 electron volts per ion.

In figure 3, it can be seen that the measured kinetic power of 0.25 watt is only 40 percent of the total power, 0.615 watt, measured at floating potential V_f. This measured power is even larger than can be calculated from the convective power density in the beam, which is the sum of the products

of the average energies for ions and electrons and their respective currents $j_i A_p(V_o + \varphi_i - \varphi_\omega) + j_e A_p(\frac{3}{2} T_e + \varphi_\omega)$; at V_f, $j_i = j_e$. The extra power $j_e A_p[(V_f - V_p) + \frac{1}{2} T_e]$ comes from the plasma electrons. In traversing the sheath, each electron loses the energy $e(V_f - V_p)$ that each ion gains, and it delivers an average of $2T_e + \varphi_\omega$ to the probe surface. This extra power, 0.187 watt in this case, is extracted from the local electron gas, which is supported by the discharge. Therefore, a floating calorimeter power measurement in a tenuous plasma beam is larger than the product of the convective power density in the beam and calorimeter area.

RESULTS AND DISCUSSION

Discharge Noise

To put the results in the proper perspective, it is first necessary to discuss the discharge noise, which was quite large. Most potential measurements were made with dc meters. Figure 4 presents the emissive probe measurement of plasma potential displayed on an oscilloscope. This measurement was made at the noisiest point, which was just ahead of the front coil in the conical anode area. The noise has a maximum peak-to-peak amplitude of 25 volts about a dc signal of approximately 87 volts. These are significant fluctuations compared to the total acceleration of 70 volts, but they are not believed to have a major effect on the conclusions of the investigation.

Ion Acceleration

The results of several plasma potential surveys using an emissive probe are presented in figure 5. The potentials were determined with a $1.5.10^{+6}$-ohm voltmeter, which read an average value of the fluctuating plasma potential previously discussed. It was necessary to use an emissive probe to obtain a

reasonable determination of the shape of plasma equipotential lines, since floating potentials for a nonemitting probe were also measured and did not show similar profiles. The probe floated about 20 volts below ground on axis, but it floated 20 to 50 volts above ground off axis, which would indicate a trough of low potential down the center of the exhaust beam. These low-floating voltages were evidently caused by high-energy electrons, which were detected by the calorimetric probe. To drive the Langmuir calorimetric probe into the ion saturation region required a potential of 200 volts below ground on axis, but off axis, ion saturation current was obtained at only 20 to 30 volts below ground.

The cathode jet area on axis and extending a little beyond the cylindrical portion of the anode could not be probed because of the extreme heat fluxes in that area. The jet was interesting in that its end was fairly well defined. The thrustor axis could be probed to within about 1/4 inch of the end of the cathode jet with very little heating. If the probe was translated that last quarter inch, however, its tip would heat to a bright yellow, and the 99^{+}-percent aluminum-oxide ceramic would melt. The jet was also fairly well defined radially. Probes could be placed within a radius of about 0.1 to 0.15 inch without excessive heating.

The equipotential lines are essentially perpendicular to magnetic flux lines. This indicates that Hall currents are not important, since Hall current acceleration requires equipotential lines to coincide roughly with flux lines. Also, the accelerating voltage drop appears to take place over large distances compared to a Debye distance, indicating that acceleration is accomplished in a relatively space charge free plasma. In addition,

the equipotential lines are fairly circular inside the anode and even eliptical outside, indicating that the beam is at least spherically diverging. The equipotential map, therefore, indicates that the discharge current does not participate directly in acceleration, as it does in a Hall current accelerator, and that plasma is relatively space-charge neutral. Both these conclusions support the method of ion acceleration proposed in the INTRODUCTION.

To further investigate this acceleration process, an axial survey downstream of the anode was made on axis using Langmuir and emissive probes to determine electron pressure and plasma potential. The results are shown in figure 6. The 56-volt point was obtained by linearly extrapolating the logarithm of the probe current to the plasma potential measured by the emissive probe. The extrapolation was based on the semilog probe characteristic slope near floating potential, and it required spanning about a decade in probe current to reach the measured plasma potential. This was necessary because the probe trace indicated a premature saturation which may be due to the magnetic field. The other points were unaffected by that problem. The variation of pressure with voltage, shown in figure 6, is what would be expected for an electron gas with a Maxwellian energy distribution temperature of 7.4 electron volts. The temperatures from Langmuir probe measurements are presented in figure 6 and, in the range between 33 and 56 volts, are in fair agreement with this temperature.

In reference 1, an interesting relation in the collisionless limit was obtained directly by combining the electron and ion momentum equations and by assuming singly ionized ions, approximate charge neutrality, and no axial current flow. Then, on the axis of symmetry,

$$E_Z = - \frac{1}{qn} \frac{\partial Pe}{\partial Z} \qquad (3)$$

The exponential dependence of the pressure on voltage shown in figure 6 satisfies this equation for a constant electron temperature of 7.4 electron volts. The measured temperature was very close to that at higher voltage and changed only 25 percent over the measured range. This agreement between the measured pressure variation with voltage and equation (3) indicates that the ion-accelerating electric field is supported by the electron pressure gradient.

Verification of Thrustor Performance

In order to verify the thrustor performance, the average ion energy in the beam was surveyed with the Langmuir calorimetric probe at the plane indicated in figure 5. These results are presented in figure 7 and show that the beam had spread rapidly ahead of the survey plane. The ion current was integrated to get the total accelerated current, which was 0.58 ampere. This, when compared with the mass flow of 0.355 milligram per second of argon or 0.86 ampere, gives a propellant utilization of 67 percent, which is higher than might be expected considering the modest performance.

If the energy per ion in electron volts is referenced to ground, the value will indicate the average potential of the region in which the ions were formed. This potential is presented in the upper curve, and it can be seen that near the axis, the ions all came from a potential of better than 90 volts, which was inside the cylindrical portion of the anode on the equipotential plot. The data at the edges indicate even higher energy, which is believed due to inaccuracy of small power measurement at

low probe ion currents and input powers. The plasma potential as determined by an emissive probe is presented in the lowest curve. The local ion energy in electron volts is the increment between the source potential and plasma potential curves. To check that the ions were all formed inside the anode, and therefore had kinetic energy of about 72 electron volts per ion, the measured current density and velocity corresponding to 72 electron volts per ion were used to calculate a local number density of 2.16×10^{16} meters^{-3} on the centerline. This is the identical value determined there during another run from the electron saturation portion of a Langmuir probe characteristic. This agreement, which is considerably better than the accuracy of the data, again indicates that the portion of the beam with significant kinetic energy consists of ions originating inside the thrustor anode.

Since all the ions appeared to originate near the maximum voltage, it was assumed that ions at all radii had an equal energy of 72 electron volts. Then the ion momentum was integrated, using the measured ion current density, out to a radial distance about three times the anode exit radius. A cosine correction was made at large radii to correct for momentum direction. This gave a total ion momentum rate of 4.18×10^{-3} newton, which compares rather well with the thrust stand measurement of 3.83×10^{-3} newton. As will be seen later, the electron pressure integrated over this same area is 0.36×10^{-3} newton. This, added to the ion momentum flux, makes the thrust calculated by integrating around a momentum contour at this plane about 18 percent greater than the measured thrust, which is probably within the accuracy of the data. The ion momentum responsible for the thrust of the magnetic expansion thrustor therefore, appears fairly close to the thrustor

exit as momentum of ions which originated inside the anode. Therefore, the entrainment of background gas probably does not play a significant part in thrust production at the conditions of this test.

Electron Pressure Forces on the Thrustor

The force on the expanding magnetic field is due to its radial containment of the electron gas. Macroscopically, the electron pressure force arises from the interaction of the radial magnetic field with the azimuthal current associated with a radial density gradient of electrons orbiting around magnetic field lines. This azimuthal current is similar to the magnetization current of magnetic field theory. To determine this force would require taking the derivative of data, which would probably introduce sizable errors. Therefore, the problem was approached microscopically by integrating the axial magnetic mirror force on an orbiting electron $(m_e v_e^2 \sin^2 \theta/2B)(\partial B/\partial Z)$ over a Maxwellian distribution. This gives an axial body force on the magnetic field per unit volume F parallel to the local magnetic field of

$$F = P_e \frac{1}{B} \frac{\partial B}{\partial Z} \tag{4}$$

where P_e is the local electron pressure, B the magnetic field, and Z the distance along a flux line. Since the pressure appears directly in equation (4), it was used to determine a representative force on the magnetic field.

Figure 8 presents lines of equal electron gas pressure as determined by Langmuir probes. Inside the anode, the probe characteristics were distorted. It was, therefore, possible to reliably determine electron gas pressure only

in front of the anode. Results of integrating to obtain the total pressure force at a plane are shown. At the anode lip the pressure force is 0.67×10^{-3} newton, and this reduces about in half to 0.36×10^{-3} newton at the calorimeter survey plane.

In order to estimate the previously derived force on the magnetic field, it was decided to determine the total force on a 0.0508-inch-diameter cylinder extending from the plane of the front coil to the plane of the calorimetric survey, 0.14 meter downstream. This cylindrical volume started at the front magnet because the magnetic field was symetrical between the coils, which should produce nearly canceling forces in the interior region. The cylinder radius was chosen large enough to include most of the areas of significant electron pressure and small enough to minimize the errors due to using the on-axis value of $(1/B)(\partial B/\partial Z)$ and ignoring that the body forces are parallel to the local flux lines and not axial. To calculate the force, the pressure was averaged over the cross sectional area, and the on-axis value of $(1/B)(\partial B/\partial Z)$ was assumed to apply throughout the volume. The variation of electron gas pressure and $(1/B)(\partial B/\partial Z)$ with axial distance are presented, respectively, in parts (a) and (b) of figure 9. The product of these two variables with the cross sectional area of the assumed cylinder 2.02×10^{-3} square meter is the force per meter on the cylindrical volume and is presented in figure 9(c). The area under this curve can then be integrated to give an electron gas force on the magnetic field of $1.74.10^{-3}$ newton, which is about half of the measured thrust. This is not expected to be an accurate calculation but only an indication of the proper order of the force on the magnetic field. Unfortunately, the pressures in the thrustor could not be measured, so that

the force on the back plate could not be determined. The interesting aspect of both this force and the pressure force on the structure is that it doesn't really require any ion acceleration, but only a quiescent electron gas to be present in the thrustor and expanding magnetic field. Therefore, this could be a source of anomalous thrust when the magnetic expansion engine is operated at a higher background density.

CONCLUDING REMARKS

The exhaust beam of a magnetic expansion thrustor was investigated to determine the mechanism of the thrust production and to obtain a separate confirmation of performance. The equipotential profiles in the beam indicated that Hall currents were not important and that the acceleration was obtained in a relatively space-charge-neutral region. Langmuir calorimetric probe measurements, 0.10 meter downstream of the thrustor, indicated that only ions were accelerated, and they originated well up inside the anode. The thrust, therefore, appeared to be produced by ionizing the propellent well up inside the anode and accelerating the ions in a charge neutral region. Assuming that the ion acceleration and transmission of thrust from the plasma to the thrustor were accomplished by an essentially quiescent electron gas produced results that appeared reasonable. In front of the thrustor where electron pressure could be measured, the ion accelerating electric field E_Z was found to be supported by an axial electron pressure gradient, satisfying the momentum considerations corresponding to this accelerator model. The electron gas force on the structure could not be determined. However, the axial force of the contained electron gas on the expanding magnetic field was calculated and found to be about half of the measured thrust. The

magnetic expansion thrustor, therefore, appears to obtain its thrust by supporting a hot quiescent electron gas, which ionizes the propellent and accelerates it in a relatively space-charge-neutral region.

REFERENCES

1. Seikel, G. R., Bowditch, D. N, and Domitz, S., "Application of Magnetic-Expansion Plasma Thrustors to Satellite Station Keeping and Attitude Control Missions", AIAA Paper 64-677 (August 1964).

2. Pinsley, E. A., Walch, A. P., Banas, C. M., Davis, J. W., and Churchill, T. L., "Applied Research on the Oscillating-Electron Ion Engine", United Aircraft Corp., Rep. No. B910065-9 (AFASD-TDR-63-253) April 1963.

3. Miller, D. B. and Bethke, G. W., "Cyclotron Resonance Thruster Design and Diagnostics Techniques", AIAA Paper 65-301 (July 1965).

4. Ahmed, S. A. and Hendel, H. W., "Space Charge Acceleration of Ions at Electron Cyclotron Resonance", AIAA Paper 64-24 (January 1964).

5. Ducati, A. C., Giannini, G. M., and Muehlberger, E., "High Specific Impulse Thermo-Ionic Acceleration", AIAA Paper 64-668 (August 1964).

6. Cann, G. L., Moore, R. A., and Giltner, G. H., "Lithium Plasma Thrustor Performance", AIAA Paper 65-295 (July 1965).

7. Bennett, S., Enos, G., John, R. R., and Tuchman, A., "MPD Arc Jet Engine Performance", AIAA Paper 65-296 (July 1965).

8. Patrick, R. M. and Powers, W. E., "Plasma Flow in a Magnetic Annular Arc Nozzle", Advanced Propulsion Concepts (Gordon and Breach Sci. Pub. Inc., 1963), Vol. I, p. 115.

9. Brockman, P., Hess, R., Bowen, F., and Jarrett, O., "Diagnostic Studies in a Hall Accelerator at Low Exhaust Pressure", AIAA Paper 65-297 (July 1965).

10. Jones, R. E., and Walker, E. L., "Status of Large Vacuum Facility Tests of an MPD Arc Thrustor", AIAA Paper 66-117 (January 1966).

11. Domitz, S., "Experimental Evaluation of a Direct-Current Low Pressure Plasma Source", NASA TN D-1659 (April 1963).

12. Compton, K. T., "On the Theory of the Mercury Arc", Phys. Rev. 37, 1077-1090 (May 1931).

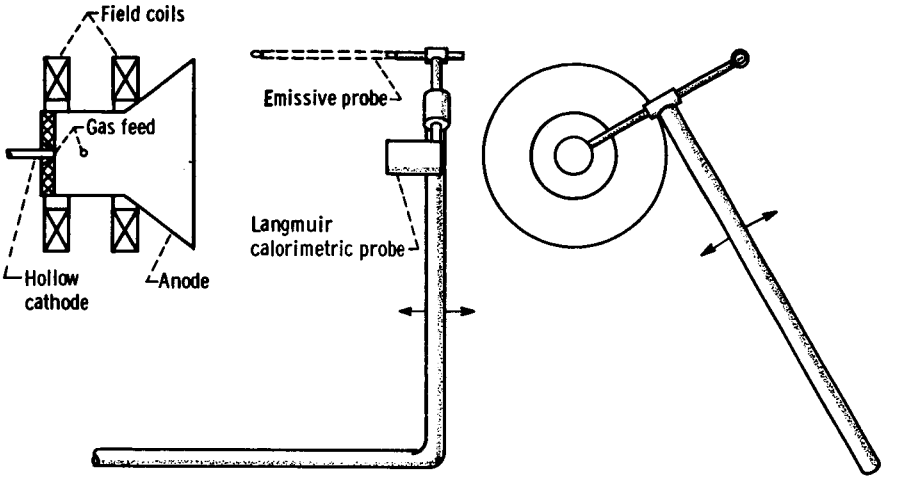

(a) Side view. (b) Axial view.

Figure 1. - Magnetic expansion thrustor and probe actuation system.

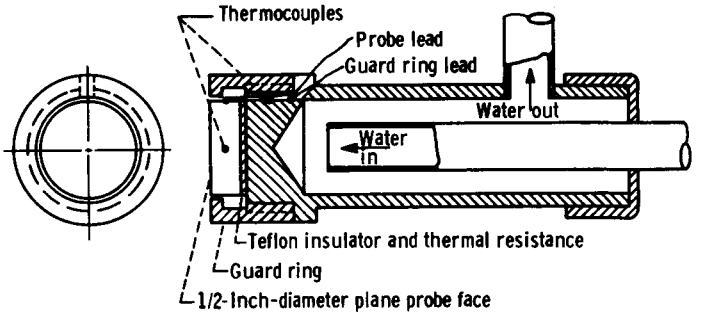

(a) Langmuir calorimetric probe.

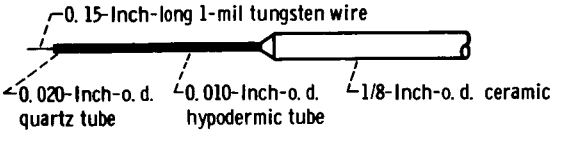

(b) Langmuir probe.

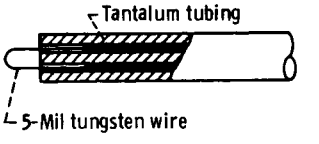

(c) Emitting probe.

Figure 2. - Plasma probes used during investigation.

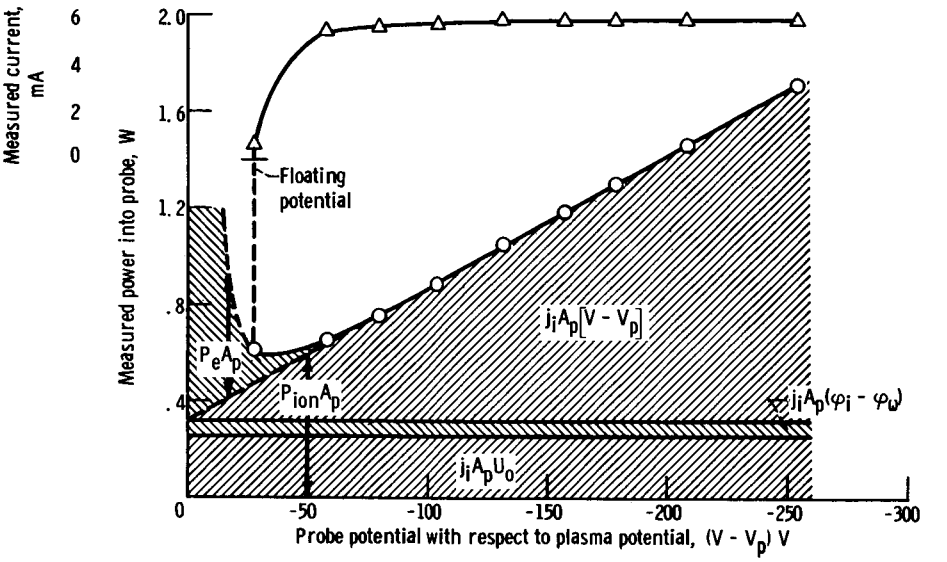

Figure 3. - Probe characteristics of power and current versus potential.

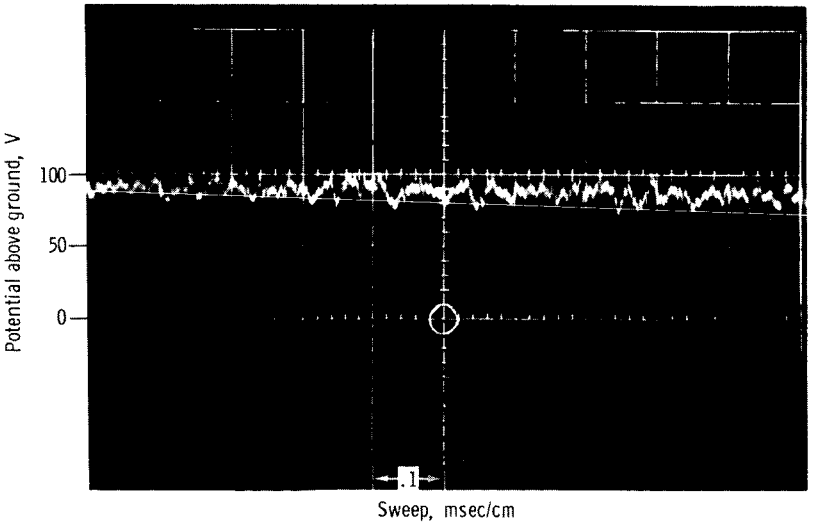

Figure 4. - Noise on emissive probe measurement of plasma potential, 0.025-meter inside anode lip.

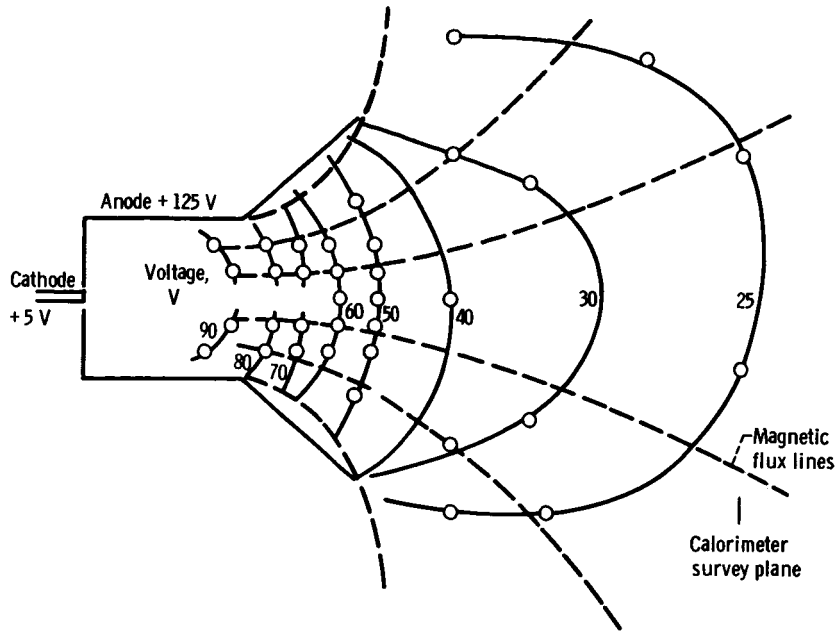

Figure 5. - Plasma potential profiles determined by an emitting probe.

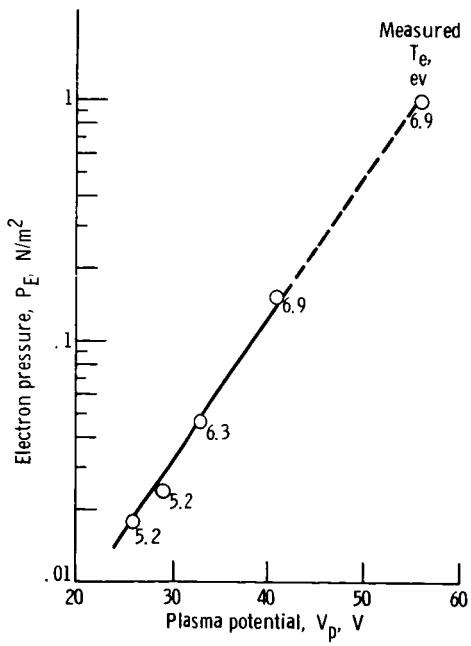

Figure 6. - Relation between electron gas pressure and plasma potential on the thrustor axis. Data obtained with Langmuir and emissive probes.

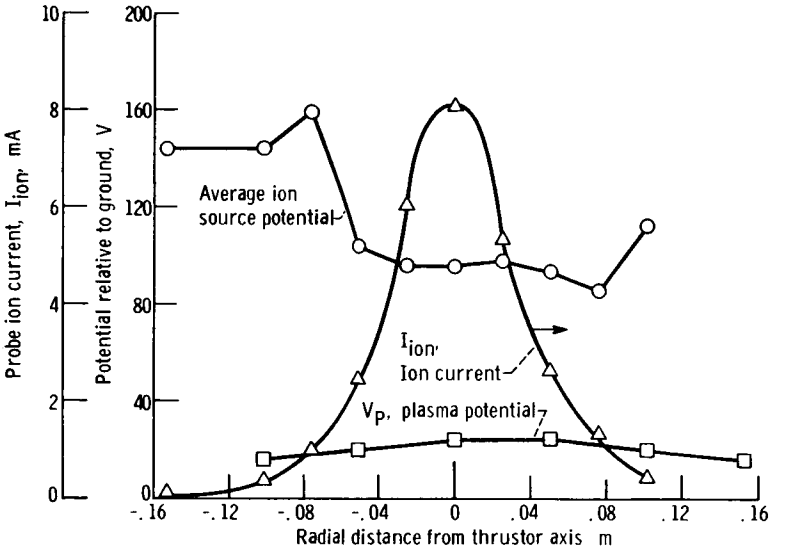

Figure 7. - Ion current and source potential profiles; anode potential = 125 V, measured thrust = 3.83×10^{-3} N.

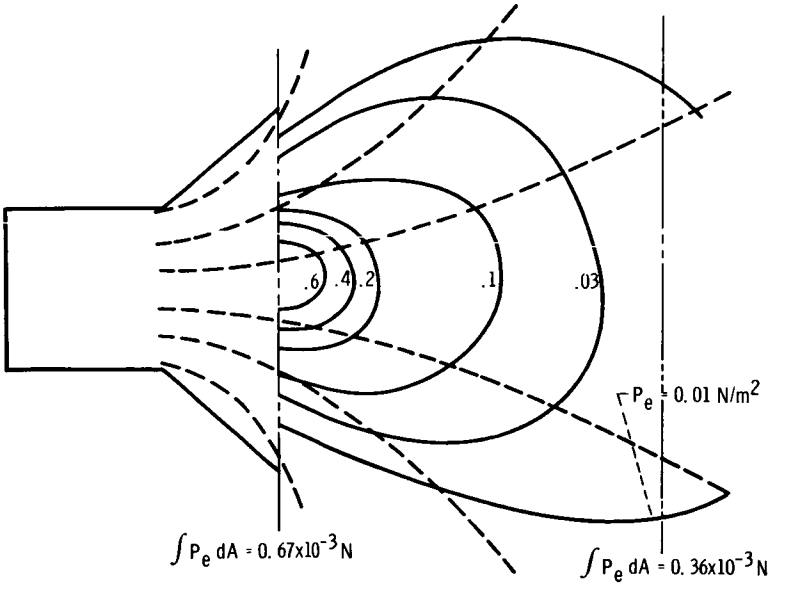

Figure 8. - Electron gas pressure profiles as determined by Langmuir probe measurements.

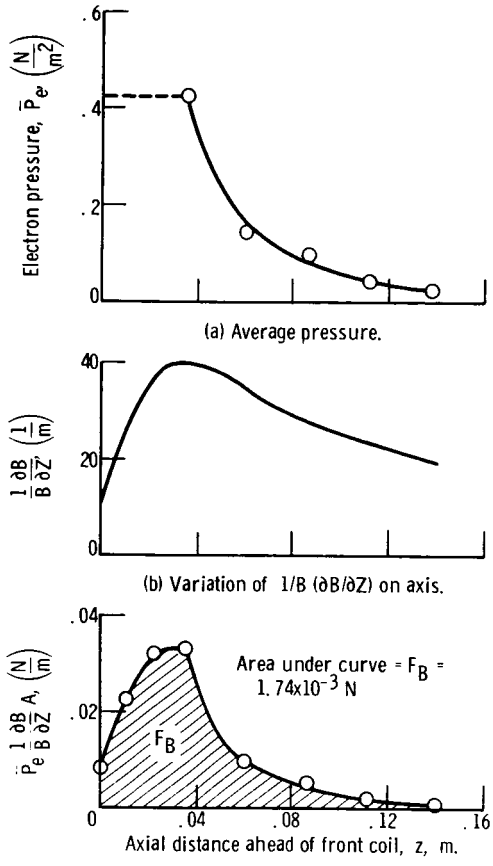

Figure 9. - Evaluation of electron gas pressure force on magnetic field for cylindrical volume of 0.0508 diameter and 0.14 m long.